JOURNAL OF THERMOPHYSICS AND HEAT TRANSFER
Vol. 17, No. 2, April–June 2003

Prediction of Minimum Heat Flux for Water Jet Boiling on a Hot Plate

Zheng-Hua Liu*
Shanghai Jiaotong University, 200030 Shanghai, People's Republic of China

A theoretical analysis was carried out for predicting the minimum heat flux (MHF) point of boiling curves for water jet impingement boiling on the horizontal high-temperature plate at the jet stagnation zone with the same size as the nozzle. Simplified two-phase flow boundary-layer equations were used to derive a limiting flow condition of the steady vapor layer, and from it the qualitatively theoretical equations were obtained for predicting the MHF point. The equations factors were determined from the experimental data presented by the author and other researchers. Semitheoretical correlations were proposed for predicting the wall superheat and the MHF at the MHF point, and these correlations agreed with existing experimental data.

Nomenclature

a = empirical correlation factor
c_p = specific heat, $J \cdot kg^{-1}\ K^{-1}$
d = diameter of nozzle, m
f = empirical correlation factor
h_{fg} = latent heat of evaporation, $J \cdot kg^{-1}$
h'_{fg} = modified latent heat of evaporation, $h_{fg} + c_{p,v}[(T_w + T_{\text{sat}})/2 - T_{\text{sat}}]$, $J \cdot kg^{-1}$
Nu = Nusselt number
P = pressure, Pa
Pr = Prandtl number
q = heat flux, $J \cdot m^{-2}\ s^{-1}$
Re = Reynolds number
r = radial coordinate, m
T = temperature, K
u = velocity in the radial direction, ms^{-1}
V = velocity in the vertical direction, ms^{-1}
y = vertical coordinate, m
y' = vertical coordinate (Fig. 1b), m
α = heat transfer coefficient, $J \cdot m^{-2}K^{-1}\ s^{-1}$
δ = thickness of boundary layer, m
λ = thermal conductivity, $J \cdot m^{-1}K^{-1}\ s^{-1}$
μ = viscosity, $Pa \cdot s$
ν = kinematic viscosity, m^2s^{-1}
ρ = density, $kg \cdot m^{-3}$
τ = interface stress, Pa

Subscripts

a = atmospheric
l = liquid
M = minimum heat flux point
r = radiation
s = stagnation
sat = saturated
sub = subcooled
t = temperature or thermal
v = vapor
w = wall
δ = vapor–liquid interface
0 = initial position at the exit of nozzle
∞ = mainstream zone of liquid flow

Received 1 August 2001; revision received 19 September 2002; accepted for publication 28 October 2002.

*Professor, School of Mechanical and Power Engineering; liuzhenh@guomai.sh.cn.

Introduction

WATER jet impingement cooling has been widely used as a highly effective cooling method in the iron and steel industry, such as in hot-rolling, continuous costing, and forging processes. In accord with the temperature ranges of the heat transfer surface, the heat transfer modes may be divided into forced convection, nucleate boiling, transition boiling, and film boiling.[1–12] In particular, it is very important to understand the heat transfer characteristics of film boiling and transition boiling for actual cooling processes of hot strip mills.

For forced convective heat transfer of water jets, a great variety of theoretical and experimental studies have been reported in the open literature.[1–5] Miyazaki and Siberman[6] and Watson[7] carried out numerical studies on velocity distributions and forced convective heat transfer characteristics.

For nucleate boiling of water jets, many experimental investigations have been conducted to understand the boiling heat transfer characteristics of water or liquid freon jet flow.[8–10] Ma and Bergles[11] carried out an experiment studying jet impingement nucleate boiling for a small hot surface. Kumagai et al.[12,13] experimentally investigated transition boiling heat transfer characteristics of two-dimensional water jet flow on a large flat plate. In addition, Katto and Yokoya[14] and Monde and Mitsutake[15] proposed several correlations for prediction of the critical heat flux for liquid jet impingement boiling on large heated disk surfaces.

These researchers[8–15] found that, when transition or film boiling occurs on a high-temperature plate whose scale is much larger than the scale of the jet nozzle, the liquid flow has broken, and the whole cooling zone is divided into a jet stagnation zone (black zone) and a mist cooling zone (drying zone). In the jet stagnation zone, a mainstream liquid layer flows above a steady vapor layer. In the mist cooling zone, the liquid layer and the vapor layer break up and become a mist flow, which consists of liquid drops and vapor. In this case, the wall temperatures and the local heat transfer coefficients would strongly vary along the flow direction; hence, measurement of the wall temperatures and wall heat fluxes are very difficult.

Most previous studies for water jet impingement boiling focused on the nucleate boiling region and the critical heat flux point because the sizes of the jet nozzles were much smaller than those of the heat transfer surfaces in these studies. The experimental data in transition and film boiling regions is insufficient.

Limited work has been reported for film boiling of water jet impingement on a stagnation zone having the same size as the nozzle. In this case, both wall heat fluxes and wall temperatures are uniform on the entire heat transfer surface.[16–18] Ishigai et al.[16] carried out an experimental study for film boiling heat transfer of two-dimensional water jets. Nakanishi et al.[17] experimentally investigated the transition and film boiling heat transfer characteristics of a two-dimensional water jet in detail and proposed an empirical correlation for the minimum heat flux (MHF) data. These studies investigated mainly the effects of the primary governing parameters, that is, the subcooling and impact velocity of the water, on the film boiling heat transfer. Most recently, Liu and Wang[18] conducted a theoretical and experimental study for the film boiling heat transfer characteristics of water jets in the stagnation zone and proposed a semitheoretical correlation for predicting the film boiling heat transfer coefficients.

For water jet impingement boiling on a hot plate, the assessment of the MHF point is very important in the two different boiling regions of transition and film boiling. The assessment of the MHF point is also difficult and has not been systematically studied yet. Previous modeling techniques used for the MHF point in pool boiling or convective boiling in crossflow can be grouped into two major categories: 1) the thermophysics model or the temperature controlled model and 2) the hydrodynamic instability model or the heat-flux controlled model. In the former model, the MHF-point temperature is regarded as the dominant factor that determines the MHF point, and thus, the value of the MHF-point temperature is analyzed. The MHF-point temperature is related to the so-called maximum wetting temperature where liquid–solid contact can occur.[19,20] A typical model of this kind is the foam limit model proposed by Spiegler et al.[19] In the latter model, the minimum heat flux is related to a type of critical energy density. The Kelvin–Helmholtz instability wavelength is used to determine the length scale of the vapor film unit, and from it, the minimum heat flux can be obtained. Typical models of this type are the hydrodynamic instability models proposed by Zuber,[21] Berenson,[22] Lienhard and Wang, [23] and Lienhard and Dhir.[24]

In this study, a new, special approach was adopted to clarify the MHF-point flow condition. A simplified two-phase flow model was used to qualitatively derive the hydrodynamic limiting condition of steady film boiling, that is, the hydrodynamic limiting condition of steady vapor layer existing on the heat transfer surface. From this model, semitheoretical correlations were obtained for predicting the MHF point. Then the correlation factors were determined experimentally from available MHF-point data proposed by the author and other researchers.

Simplified Theoretical Analysis

Film Boiling Region

Liu and Wang[18] have carried out the theoretical analysis for predicting the heat transfer coefficients for the film boiling region. However, this analytical process still needs to obtain the hydrodynamic limiting condition of steady vapor layer existing on the heat transfer surface. Figure 1a is a schematic diagram of the analytical model, Fig. 1b is a schematic diagram of the boundary layer of vapor and liquid and coordinates for the steady film boiling region, and Fig. 1c illustrates the limiting flow condition of the vapor layer and liquid layer at the MHF point. Here, a round water jet of diameter d impinges vertically on a circular flat plate, with an initial jet velocity V_0 and an initial water temperature T_0 at the exit of nozzle. For film boiling on a high-temperature flat plate, the heated surface can be divided into a central jet stagnation zone and a surrounding mist cooling zone. In this study, only the stagnation zone is considered with the analytical region defined as $0 \le r \le d/2$. If the impinging velocity or the stagnation velocity on the heat transfer surface is used as the flow parameter, instead of the outlet velocity at the jet nozzle, the influence of the jet height needs not be considered. In the stagnation zone, vapor forms a very thin layer on the heated surface, and the vapor–liquid interface is assumed to be smooth. The thickness of vapor layer is so thin that the inertial forces and the pressure differences in the vertical direction can be neglected, whereas the temperature distribution is linear in the vapor layer. This simplified modeling technique is similar to the well-known Nusselt analysis for laminar film condensation on a vertical plate. We assumed here that no coupling relation exists between the radiative and the convective heat transfer, such that the radiative heat transfer can be calculated independently as with the Bromley et al. treatment.[25]

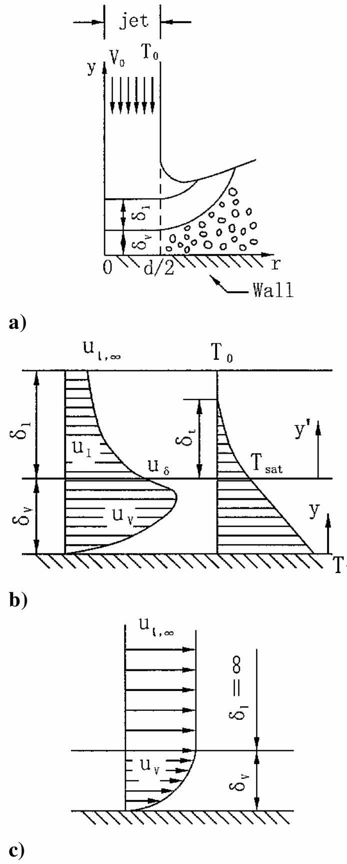

Fig. 1 Schematic diagrams of the physical model and coordinate system: a) analytical zone, 0 ≤ *r* ≤ *d*/2, b) boundary layer of vapor and liquid for steady film boiling region, and c) limiting flow condition of the vapor layer at the MHF point.

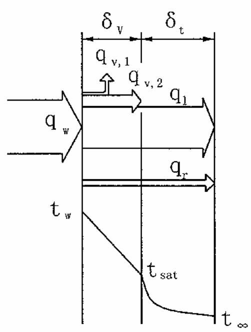

Fig. 2 Schematic diagrams of the heat flux distribution.

Figure 2 is a schematic diagram of the heat flux distribution. The wall heat flux can be divided into three parts, that is,

$$q_w = q_v + q_l + q_r \tag{1}$$

In part 1, q_v is used for the superheating for the generated vapor, $q_{v,1}$, and the evaporation for the liquid, $q_{v,2}$. The former is secondary compared with the latter, and its effect can be neglected or included in a modified latent heat. In part 2, q_l is used for the heat transfer into the subcooled liquid. In part 3, q_r is the radiative heat transfer and is used for heating the subcooled liquid or for the evaporation of the saturated liquid. Here q_r can be neglected for highly subcooled liquid because it is much less than q_l.

At the interface of the velocity boundary layer of the liquid and the mainstream flow zone, the radial velocity of liquid can be described as[3]

$$u_{l\cdot\infty}/V_s = r/d \tag{2}$$

where V_s is the stagnation velocity at the center of the stagnation zone and is equal to the initial velocity at the exit of nozzle, V_0, if the effect of gravity is neglected.

When it is assumed that the vapor layer does not affect the pressure profile and velocity distribution in the mainstream liquid flow zone, then at the vapor–liquid interface $y = \delta_v$ and the distribution of pressure and the radial velocity can be expressed as[6,7]

$$(P - P_a)/(P_s - P_a) = 1 - (2r/d)^2 \tag{3}$$

$$u_\delta / V_s = 2r/d \tag{4}$$

where P_s is the stagnation pressure at the center of the stagnation zone, $P_s = (1/2)\rho_l V_s^2 + P_a$, and P_a is the atmospheric pressure.

Inside the velocity and the thermal boundary layers of liquid, the distributions of velocity and temperature are taken as parabolic distributions[26] [Eqs. (2) and (4) and Fig. 1b],

$$(u_l - u_{l\cdot\infty})/(u_\delta - u_{l\cdot\infty}) = 1 - \tfrac{3}{2}(y'/\delta_l) + \tfrac{1}{2}(y'/\delta_l)^3 \tag{5}$$

$$(T_l - T_0)/(T_{\text{sat}} - T_0) = 1 - \tfrac{3}{2}(y'/\delta_t) + \tfrac{1}{2}(y'/\delta_t)^3 \tag{6}$$

where δ_l and δ_t are the thickness of the velocity boundary layer and the thermal boundary layer of liquid, respectively, and T_{sat} and T_0 are the saturation temperature at the vapor–liquid interface and the mainstream temperature of liquid, that is, the initial temperature at the exit of the jet nozzle. We take, as usual,[26]

$$\delta_t = \delta_l Pr_l^{-\frac{1}{3}} \tag{7}$$

Inside the vapor layer, the momentum equation is simplified as[26]

$$\mu_v \frac{\partial^2 u_v}{\partial y^2} = \frac{\partial P}{\partial r} \tag{8a}$$

$$y = 0, \qquad u_v = 0, \qquad y = \delta_v, \qquad u_v = u_\delta \tag{8b}$$

Integrating Eq. (8) and substituting Eqs. (3) and (4) into Eq. (8) yields

$$u_v = \left(2rV_s^2\rho_l \big/ \mu_v d^2\right)\left(y\delta_v - y^2\right) + (2rV_s/d)(y/\delta_v) \tag{9}$$

At the vapor–liquid interface $y = \delta_v$, the interfacial stress is[26]

$$\tau_\delta = \mu_v \frac{\partial u_v}{\partial y} = \mu_l \frac{\partial u_l}{\partial y'} \tag{10}$$

Substituting Eqs. (5) and (9) into Eq. (10) and defining $Re_l = V_s d/\nu_l$ then yields

$$\delta_l = \tfrac{3}{4}(\mu_l/\mu_v)\delta_v \big/ \left[Re_l(\mu_l/\mu_v)(\delta_v/d)^2 - 1\right] \tag{11}$$

At any section of the radial direction in the vapor layer, r, the vapor mass that flows out the vapor layer along the radial direction equals to the generated vapor mass from the vapor–liquid interface. This balance yields the following mass conservation equation:

$$\int_0^{\delta_v} 2\pi r \rho_v u_v \, \mathrm{d}y = \frac{\pi r^2 q_v}{h_{fg}} \tag{12}$$

The superheating effect in the vapor is neglected in Eq. (12). This simplification can be easily modified by using a modified latent heat of evaporation, $h'_{fg} = h_{fg} + c_{p,v}[(T_w + T_{\text{sat}})/2 - T_{\text{sat}}]$ instead of h_{fg}.

Substituting Eq. (9) into Eq. (12) yields

$$q_v/2h_{fg}\rho_v V_s = Re_l/3(\mu_l/\mu_v)(\delta_v/d)^3 + (\delta_v/d) \tag{13}$$

At the vapor–liquid interface, the convective heat flux through the thermal boundary layer of subcooled liquid would be (Fig. 1b)

$$q_l = -\lambda_l \frac{\partial T_l}{\partial y'}\bigg|_{y'=0} \tag{14}$$

Substituting Eqs. (6) and (7) into Eq. (14) yields

$$q_l = \tfrac{3}{2}\lambda_l \Delta T_{\text{sub}} Pr_l^{\frac{1}{3}} \big/ \delta_l \tag{15}$$

where $\Delta T_{\text{sub}} = (T_{\text{sat}} - T_0)$ denotes the liquid subcooling.

In wall heat flux q_w, both q_v and q_l pass entirely through the vapor layer (where q_v supplies the evaporative heat for the liquid at the vapor–liquid interface), reaching the vapor–liquid interface by thermal conduction. Hence, in accord with Fourier's law (see Ref. 26)

$$q_l + q_v = \Delta T_{\text{sat}}\lambda_v/\delta_v \tag{16}$$

Equations (11), (13), (15), and (16) have constructed a closed system of equations to solve for δ_v, δ_l, q_l, and q_v using a known ΔT_{sat}. Therefore, analytical solutions of film boiling heat transfer can be obtained. Here $\Delta T_{\text{sat}} = (T_w - T_{\text{sat}})$ is the wall superheat. If δ_v is taken as a known variable instead of ΔT_{sat}, then δ_l, q_l, q_v, and ΔT_{sat} corresponding to δ_v can be easily evaluated. The film boiling curves of q_w against ΔT_{sat} can be plotted. In accord with trial calculations, the range of δ_v is about 20–100 μm.

From Eqs. (11), (13), (15), and (16), δ_v, δ_l, q_l, and q_v are independent of r. Therefore, the constant wall temperature condition corresponds to the constant wall heat flux condition, and the wall temperature and the wall heat flux would be uniform in the stagnation zone.

For steady film boiling, $Re_l(\mu_l/\mu_v)(\delta_v/d)^2$ is much greater than unity. [$Re_l \approx 10^4 - 10^5$, $(\mu_l/\mu_v) \approx 30$, δ_v is on the order of several tens of micrometers, and d is several millimeters. $Re_l(\mu_l/\mu_v)(\delta_v/d)^2 > 10$.] Hence, Eqs. (11) and (13) may be simplified as

$$\delta_l = \tfrac{3}{4}\left(d^2 \big/ Re_l \delta_v\right) \tag{17}$$

$$q_v/h_{fg}\rho_v V_s = \tfrac{2}{3}(\delta_v/d)^3(\mu_l/\mu_v)Re_l \tag{18}$$

For saturated liquid, $\Delta T_{\text{sub}} = 0$, and $q_l = 0$ from Eq. (15). Therefore, from Eq. (1), $q_w = q_v + q_r$. Combining Eqs. (1), (16), and (18) yields

$$q_w = (\Delta T_{\text{sat}}\lambda_v/d)^{\frac{3}{4}}\left(\tfrac{2}{3}h_{fg}\, V_s\, Re_l\, \mu_l \big/ \nu_v\right)^{\frac{1}{4}} + q_r \tag{19}$$

For the case of a highly subcooled liquid, q_l is the dominant part in q_w. Therefore, q_v and q_r may be neglected for simplifying calculations. Combining Eqs. (16), (17), and (15) yields

$$q_w \approx q_l = \sqrt{2}Re_l^{\frac{1}{2}} Pr_l^{\frac{1}{6}} (\lambda_l\lambda_v \Delta T_{\text{sub}}\Delta T_{\text{sat}})^{\frac{1}{2}} \big/ d \tag{20}$$

For example, for the case $\Delta T_{\text{sub}} = 45$ K, $\Delta T_{\text{sat}} = 500$ K, and $V_s = 3$ m/s, $q_w \approx 1.1 \times 10^6$ W/m^2 from Eqs. (11), (13), (15), and (16), $q_l \approx 1.0 \times 10^6$ W/m^2 from Eq. (20), and $q_r < 10^4$ W/m^2. Here $q_l/q_w \approx 90\%$.

For the case of a highly subcooled liquid, Eq. (20) can be also used for two-dimensional jet flow.

The effect of interfacial waviness of the vapor layer may be modified by employing an empirical correlation factor f in Eq. (20). If f is taken to be $\sqrt{2}$, Eq. (20) becomes

$$q_w \approx q_l = 2Re_l^{\frac{1}{2}} Pr_l^{\frac{1}{6}} (\lambda_l\lambda_v \Delta T_{\text{sub}}\Delta T_{\text{sat}})^{\frac{1}{2}} \big/ d \tag{21}$$

The deviations between Eq. (21) and most experimental data presented by Liu and Wang,[18] Ishigai et al.,[16] and Nakanishi et al.[17] would be improved and limited to a range of $\pm 25\%$.

Simplified Theoretical Analysis for the MHF Point

The limiting flow condition of a steady vapor layer, that is, a condition of steady film boiling, may be deduced from Eq. (10) or Eq. (11). When τ_δ is close to zero, as shown in Fig. 1c, the vapor layer would reach its thinnest thickness limit and can no longer draw the liquid flow forward along the radial direction. For this condition, the thickness of the liquid's velocity boundary layer would reach its maximum value. Hence, the steady vapor layer would collapse, and the film boiling mode would change to the transition boiling mode. Of course, the condition of $\tau_\delta = 0$ is only a theoretical limiting condition. However, we can develop a qualitative relationship to estimate the MHF point by using this limiting condition.

In accord with the discussion just before Eq. (17), the term $Re_l(\mu_l/\mu_v)(\delta_v/d)^2$ is much greater than unity in the steady film boiling region. It would gradually reduce with decreasing ΔT_{sat} [by Eqs. (16) and (21), $\delta_v \sim \sqrt{\Delta T_{\text{sat}}}$] and is close to unity at the MHF point, corresponding to the limiting condition $\delta_l = \infty$, that is, $\tau_\delta = 0$. We assume that $Re_l(\mu_l/\mu_v)(\delta_v/d)^2$ would be a constant of order unity and independent of the jet velocity and the liquid subcooling at the MHF point. Then, the limiting condition can be expressed as

$$Re_l(\mu_l/\mu_v)(\delta_{v,M}/d)^2 = a \tag{22}$$

where a is an unknown constant and would be close to unity. At the MHF point, Eq. (11) may be rewritten as

$$\delta_{l,M} = [3\delta_{v,M}/4(a-1)](\mu_l/\mu_v) \tag{23}$$

Combining Eqs. (15) and (23) yields

$$q_{l,M} = 2(a-1)\lambda_l \Delta T_{\text{sub}} Pr_l^{\frac{1}{3}}(\mu_v/\mu_l)\Big/\delta_{v,M} \tag{24}$$

For the case of highly subcooled water, according to Eqs. (16) and (1),

$$q_{l,M} \approx q_{w,M} = \Delta T_{\text{sat},M}\lambda_v/\delta_{v,M} \tag{25}$$

Combining Eqs. (24) and (25) yields finally

$$\Delta T_{\text{sat},M} = 2(a-1)\Delta T_{\text{sub}} Pr_l^{\frac{1}{3}}(\lambda_l/\lambda_v)(\mu_v/\mu_l) \tag{26}$$

Equation (26) demonstrates that the wall superheat at the MHF-point would be only a function of the liquid subcooling and is linearly related to the liquid subcooling.

The minimum heat flux at the MHF point can be obtained from Eqs. (22) and (25):

$$q_{w,M} = (1/a)^{\frac{1}{2}}\Delta T_{\text{sat},M}\lambda_v Re_l^{\frac{1}{2}}(\mu_l/\mu_v)^{\frac{1}{2}}\Big/d \tag{27}$$

Note that Eq. (27) is a theoretical equation for $q_{w,M}(\Delta T_{\text{sat},M})$ at the MHF point. The enhancement effect of the interfacial waviness of the vapor layer on the heat transfer through the vapor layer has not been considered. If the enhanced heat transfer effect of the interfacial waviness at the MHF point is modified using a form of the correlation factor f_M, as was done in the steady film boiling region, then Eq. (27) becomes

$$q_{w,M} = f_M(1/a)^{\frac{1}{2}}\Delta T_{\text{sat},M}\lambda_v Re_l^{\frac{1}{2}}(\mu_l/\mu_v)^{\frac{1}{2}}\Big/d \tag{28}$$

For the case of saturated liquid, the wall superheat and the minimum heat flux at the MHF point can also be obtained by using the same analytical process as for the case of the highly subcooled liquid. However, because of the absence of MHF point data for saturated water jet impingement boiling, we have not discussed this case in the present study.

At the MHF point, which is also the incipient location for the film boiling region, there exists a maximum Nusselt number or a minimum thickness of the vapor layer. This Nusselt number can be expressed as [Eqs. (16) and (28)]

$$Nu_M = \frac{q_{w,M}d}{\Delta T_{\text{sat},M}\lambda_v} = d/\delta_{v,M} = \left(f_M/a^{\frac{1}{2}}\right)Re_l^{\frac{1}{2}}(\mu_v/\mu_l)^{\frac{1}{2}} \tag{29}$$

The experimental values of a and f_M may be determined from experimental results by using Eqs. (26) and (29).

Correlating and Comparing Experimental Data and Correlations

The existing data sources of the MHF point for water jet impingement on horizontal hot surfaces are given in Table 1. All experiments were performed for unsteady cooling in which a flat heated stainless steel plate was cooled rapidly by a round or two-dimensional water jet having the same size as the heat transfer surface. When these data were used, the factor a could be determined from the experimental relation between $\Delta T_{\text{sat},M}$ and ΔT_{sub} in Eq. (26), and the mixed factor $a^{1/2}/f_M$ could be obtained from the experimental relation at the MHF point of $\Delta T_{\text{sat},M}$ to $q_{w,M}$ in Eq. (29).

Figure 3 shows the results for a from Eq. (26), plotting wall superheat at the MHF point vs the correlation factor a. Figure 4 shows the results for $a^{1/2}/f_M$ from Eq. (29), plotting wall superheat at the MHF point vs the mixed correlation factor $a^{1/2}/f_M$.

From Figs. 3 and 4, the following can could be concluded:

Table 1 Data sources and experimental conditions[a]

Parameter	Reference 16	17	18
Test liquid	Water	Water	Water
Pressure, MPa	0.1	0.1	0.1
Heated surface size, mm	12 × 80	12 × 80	12 × 12
Nozzle size, mm	6.2 × 50	6.2 × 50	Φ10
Jet velocity, m/s	1–3.17	0.65–3.17	1–3
Subcooling, K	5–35	5–55	5–45
Reynolds number	$(1.8–6) \times 10^4$	$(1–6) \times 10^4$	$(3–9.6) \times 10^4$
Nozzle height, mm	Unknown	Unknown	10

[a]Unsteady cooling tests for all, stainless steel thin plate for all, and constant wall heat flux for all.

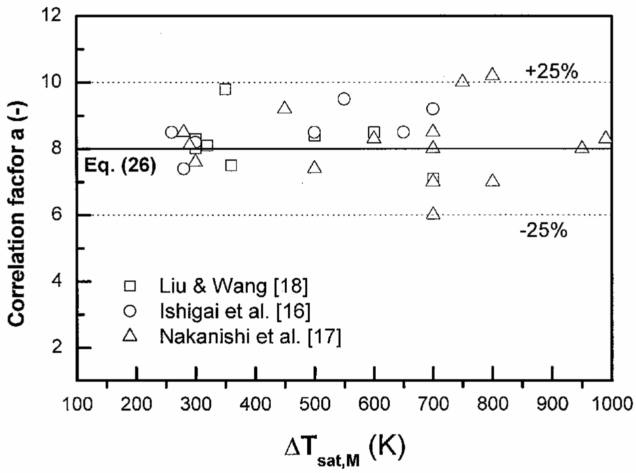

Fig. 3 Determination of correlation factor *a*.

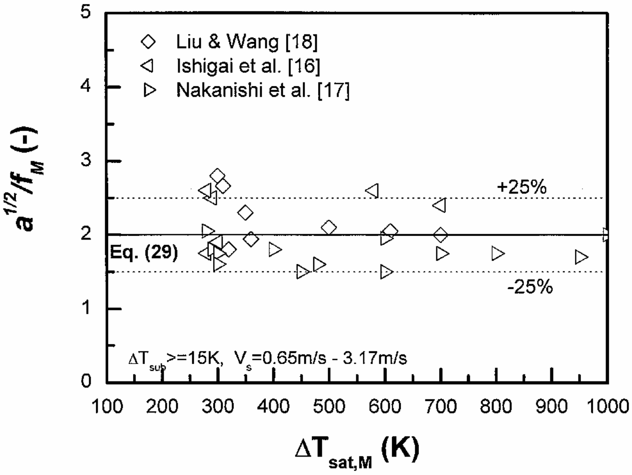

Fig. 4 Determination of mixed correlation factor, $a^{1/2}/f_M$.

1) Although there exist deviations among the data, the value of a appears to be independent of the water subcooling and water jet velocity and to vary in a narrow range from 6.0 to 10.0 in the experimental range of $\Delta T_{\text{sub}} \geq 15$ K. At most, a is a weak function of the water subcooling and water jet velocity. To simplify the predictive correlations, we take an integer value 8 as an average value of a, where the relative errors are not larger than ±25% for most of the data. This value is not obtained from a least-squares fit of all MHF point data, but by examination of Fig. 3. However, this correlating method has not caused noteworthy increases in the relative error as compared with the least-squares-fit method.

2) In the range of $\Delta T_{\text{sub}} \geq 15$ K, the values of $a^{1/2}/f_M$ appear also to be independent of the water subcooling and water jet velocity, and vary to from 1.5 to 2.8. Here, from average value taken for a, we take an integer value 2 as the average value of $a^{1/2}/f_M$, where the relative errors are not larger than ±25% for most of the data.

3) Although Eqs. (26–29) were derived for the high subcooling condition, these equations could possibly be used for relatively low subcooling, $\Delta T_{\text{sub}} = 15$ K. (See Fig. 5; there are four data points from $\Delta T_{\text{sub}} = 15$ K.) The reason may be that the vapor layer is very thin [Eq. (29)] at the MHF point, and hence q_v, used for the evaporation of the liquid, is quite small compared with q_l near the MHF point.

4) The correlated experimental results shown in Figs. 3 and 4 demonstrate the reasonability of assuming Eq. (22) as a rough approximation at the MHF point. Here a and a^2/f_M seem to be independent of the jet flow conditions from the existent experimental data. Of course, in the more accurate expressions, they should be weak functions of the jet flow conditions. If a and $a^{1/2}/f_M$ are taken as 8 and 2, then $f_M = \sqrt{2}$, which is the same as the value taken for f in the steady film boiling region [Eqs. (21) and (22)]. This is also a reason why we take the average values of a and $a^{1/2}/f_M$ as integer values.

By using the average values of a and $a^{1/2}/f_M$ from the present data, we obtain the following semitheoretical correlations from Eqs. (26) and (28):

$$\Delta T_{\text{sat},M} = 14\Delta T_{\text{sub}} Pr_l^{\frac{1}{3}}(\lambda_l/\lambda_v)(\mu_v/\mu_l) \tag{30}$$

$$q_{w,M} = 0.5\Delta T_{\text{sat},M}\lambda_v Re_l^{\frac{1}{2}}(\mu_l/\mu_v)^{\frac{1}{2}}\Big/d \tag{31}$$

When constant thermodynamic properties (which correspond to the average film temperatures of water at 80°C and vapor at 300°C) are used, Eq. (30) can be simplified to

$$\Delta T_{\text{sat},M} = 17.22\Delta T_{\text{sub}} \tag{32}$$

Nakanishi et al.[17] proposed an empirical correlation for predicting the MHF, in watts per square meter, by correlating their experimental data at the MHF point ($d = 0.0062$ m in this experiment) as

$$q_{w,M} = (5.4 + 2.846\Delta T_{\text{sub}})V_s^{0.607} \times 10^4 \tag{33}$$

When Eq. (30) is substituted into Eq. (31) and constant thermodynamic properties (which correspond to the average film temperatures of water at 80°C and vapor at 300°C) are used, Eq. (31) can be written as

$$q_{w,M} = 0.20\Delta T_{\text{sub}}(V_s/d)^{0.5} \times 10^4 \tag{34}$$

In the range of the existent experimental data[16–18] ($\Delta T_{\text{sub}} \geq 15$ K and $V_s = 0.65$–3.17 m/s), the calculated values of Eq. (34) are about 20% below the corresponding values from Eq. (33).

Figure 5 shows the experimental relationship of water subcooling and wall superheat at the MHF point and comparisons of the experimental data with Eq. (32). It is found that most data fall within a range of ±30% relative error as compared to Eq. (32). Parts of the data reported by Nakanishi et al.[17] show a trend that the wall superheat at the MHF point weakly increases with the jet velocity for highly subcooled water. Hence, the data of Nakanishi et al.[17] have a relatively greater divergence in Fig. 5 than that of the other sources.

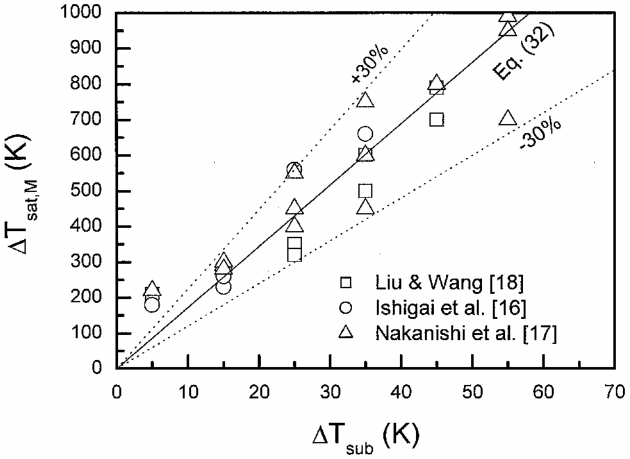

Fig. 5 Experimental results of $\Delta T_{\text{sat},M}$ vs ΔT_{sub} compared to Eq. (32).

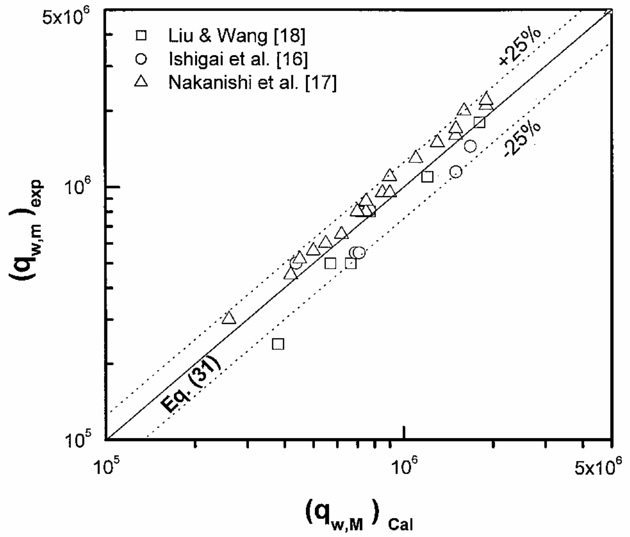

Fig. 6 Comparison between experimental data and Eq. (31) for the minimum heat flux.

Figure 6 shows the comparison of the experimental data of the minimum heat flux with the calculated values of the minimum heat flux by Eq. (31). The experimental data are in good agreement with the calculated values of Eq. (31). The relative errors of most data are less than ±25%.

Figures 7a–7c show the comparison between the experimental data of film boiling curves proposed by Liu and Wang[18] and Ishigai et al.[16] and the calculated values by Eqs. (21), (30), and (31) in the steady film boiling region and at the MHF point, respectively. The solid lines denote the calculated values from Eq. (21) for predicting the heat transfer in the steady film boiling region. The horizontal dotted lines denote the calculated values from Eq. (31) for predicting the minimum heat flux at the MHF point. The vertical or inclined broken lines denote the predicted values from Eq. (30) for the wall temperatures at the MHF point. The curves with symbols are the experimental boiling curves. On the whole, the experimental data qualitatively agree with the predictive correlations.

Because available data for the MHF point in liquid jet boiling are quite limited, the correlation factors a and $a^{1/2}/f_M$ determined in this study are approximate. Further work is needed to check and to improve the correlation factors and suggest limiting flow conditions at the MHF point. For example, the review of Nishio[27] pointed out that the wall superheat at the MHF point is basically independent of flow velocity for low and moderate velocity levels of convective boiling in crossflow. However, the MHF point will become a weak function of the flow velocity at high-velocity levels. For water jet impingement boiling, in a wider experimental range, a or f_M should be weak functions of V_s and ΔT_{sub}. However, the important

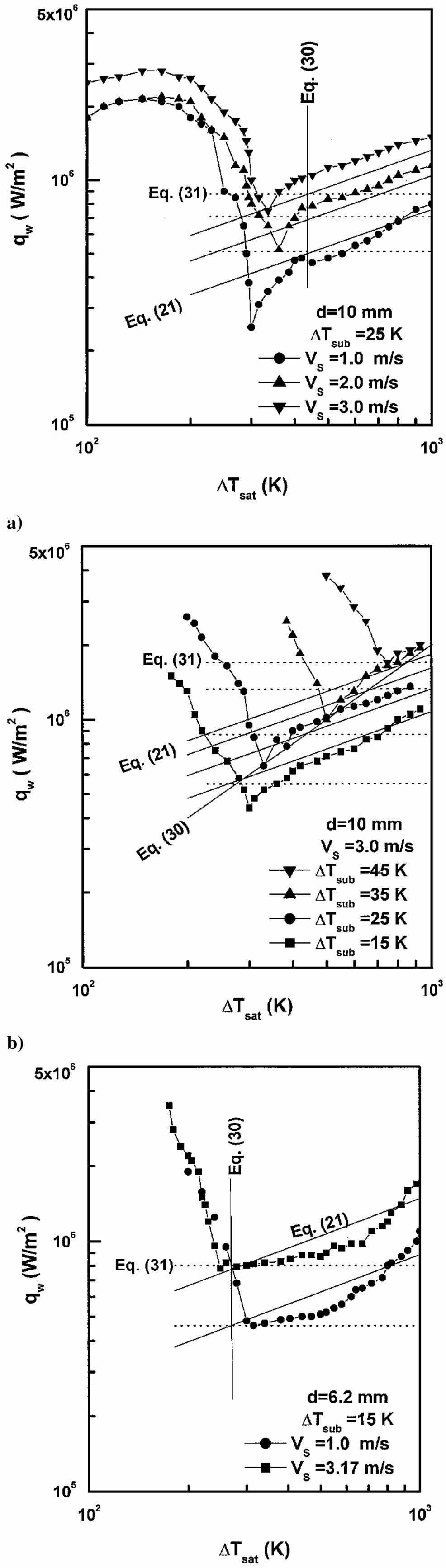

Fig. 7 Comparison between experimental data and various predictive correlations for the MHF point and the film boiling region: a) constant water subcooling case $\Delta T_{\text{sub}} = 25$ K, data from Liu and Wang,[18] b) constant jet velocity case, $V_s = 3$ m/s, data from Liu and Wang,[18] and c) constant water subcooling case, $\Delta T_{\text{sub}} = 15$ K, data from Ishigai et al.[16]

mechanisms determining the MHF point are the same, and the analytical process would also be the same as that used in the present work. Until now, all of the data concerning jet impingement transition and film boiling were obtained indirectly from the cooling curves in unsteady cooling experiments. For a rapid cooling process, the region around the MHF point is very unstable and is measured over a very short cooling period. The collapse of the vapor layer could be affected by various acoustical disturbances. Hence, great deviation of the MHF point data is unavoidable, and an exact correlation of such experimental data is difficult.

Conclusions

1) A simplified model was adopted for predicting wall superheat and the MHF point for water jet impingement boiling on a flat hot plate in the jet stagnation zone. Experimental data reported by the author and other researchers were used to obtain the correlating factors in the semitheoretical correlations. The range of applicability for this study is $\Delta T_{\text{sub}} \geq 15$ K and $V_s \leq 3.17$ m/s.

2) Water subcooling ΔT_{sub} provides a strong effect on the MHF point. For the case of highly subcooled water, the wall superheat at the MHF point $\Delta T_{\text{sat},M}$ is basically linearly dependent on ΔT_{sub}. The correlation of $\Delta T_{\text{sat},M}$ with ΔT_{sub} is expressed by Eq. (30).

3) Minimum heat flux $q_{w,M}$ is a function of $\Delta T_{\text{sat},M}$ (or ΔT_{sub}), the jet velocity, and the diameter of the jet's nozzle (or the width of the jet's nozzle for two-dimensional jet flow). At the MHF point, the correlation of $q_{w,M}$ with $\Delta T_{\text{sat},M}$ is expressed by Eq. (31).

4) Correlation factors a and a^2/f_M seem to be independent of the jet flow conditions from the existent experimental data. In the more accurate expressions, they should be weak functions of the jet flow conditions. Further work is needed to check and improve the application of the suggested correlating equations.

Acknowledgment

This work was supported by the National Natural Science Foundation of the People's Republic of China under Grant 50176029.

References

[1] Lamvik, M., and Iden, B. A., "Heat Transfer Coefficient by Water Jets Impingement on a Hot Surface," *Proceedings of 7th International Heat Transfer Conference*, Hemisphere, Washington, DC, 1982, pp. 369–375.

[2] Natsuo, H. K., Okada, J. I., and Takuda, H., "Predictable Modeling for Cooling Process of Hot Steel Plate by a Laminar Water Bar," *Umformtechnik*, Vol. 55, No. 4, 1984, pp. 143–148.

[3] Sparrow, E. M., "Analysis of Flow Field and Impinging Heat/Mass Transfer Due to a Nonuiform Slot Jet," *Journal of Heat Transfer*, Vol. 97, No. 2, 1975, pp. 191–197.

[4] Kunioka, K., Hirata, K., and Sugiyama, S., "Study on Impinging Water Cooling of Hot Plate," *Transactions of the Japan Society of Mechanical Engineers*, Ser. B, Vol. 45, No. 390, 1979, pp. 279–285.

[5] Han, M. C., Yoo, S., Yang, G., Lee, J. S., and Son, D. R., "Measurements of Impinging Jet and Heat Transfer on a Semi-Circular Concave Surface," *International of Journal Heat and Mass Transfer*, Vol. 43, No. 10, 2000, pp. 1811–1822.

[6] Miyazaki, H., and Siberman, E., "Flow and Heat Transfer on a Flat Plate with a Two-Dimensional Laminar Jet Issuing from a Nozzle of Finite Height," *International Journal of Heat and Mass Transfer*, Vol. 15, No. 8, 1972, pp. 2097–2107.

[7] Watson, E. J., "The Radial Spread of a Liquid Jet over a Horizontal Plate," *Journal of Fluid Mechanics*, Vol. 20, No. 3, 1964, pp. 481–489.

[8] Vader, D. T., Incropera, F. P., and Viskanta, R., "An Experimental Study of Cooling Characteristics for Water Jet Impinging on a Strip Mill," *Experimental Thermal and Fluid Science*, Vol. 4, No. 1, 1991, pp. 1–5.

[9] Vader, D. T., Incropera, F. P., and Viskanta, R., "Convective Nucleate Boiling on a Heated Surface Cooled by an Impinging Planer Jet of Water," *Journal of Heat Transfer*, Vol. 114, No. 1, 1992, pp. 152–157.

[10] Walf, D. H., Incopera, F. P., and Viskanta, R., "Local Jet Impingement Boiling Heat Transfer," *International Journal of Heat and Mass Transfer*, Vol. 39, No. 7, 1996, pp. 1395–1406.

[11] Ma, C. F., and Bergles, A. E., "Jet Impinging Nucleate Boiling," *International Journal of Heat and Mass Transfer*, Vol. 29, No. 4, 1986, pp. 1095–1101.

[12] Kumagai, S., Sano, T., Kamata, T., Suzuki, S., and Kubo, R., "Boiling Heat Transfer to an Impinging Jet in Cooling a Hot Metal Slab," *Transactions of the Japan Society of Mechanical Engineers*, Ser. B, Vol. 60, No. 570, 1994, pp. 259–263.

[13]Kumagai, S., Sano, T., Kamata, T., Suzuki, S., and Kubo, R., "Transient Cooling of Hot Metal Plate with Impinging Water Jet," *Transactions of the Japan Society of Mechanical Engineers*, Ser. B, Vol. 61, No. 590, 1995, pp. 351–355.

[14]Katto, Y., and Yokoya, S., "Critical Heat Flux on a Disk Heater Cooling by a Circular Jet of Saturated Liquid Impinging at the Center," *International Journal of Heat and Mass Transfer*, Vol. 31, No. 2, 1988, pp. 219–227.

[15]Momde, M., and Mitsutake, Y., "Critical Heat Flux in Forced Convective Subcooled Boiling with Multiphase Impinging Jets," *Journal of Heat Transfer*, Vol. 117, No. 2, 1996, pp. 241–243.

[16]Ishigai, S. K., Nakanishi, J. K., and Hikoshichi, T. A., "Boiling Heat Transfer for a Plane Water Jet Impinging on a Hot Surface," *Proceedings of the 6th International Heat Transfer Conference*, Vol. 1, Hemisphere, Washington, DC, 1978, pp. 445–450.

[17]Nakanishi, J. K., Ishigai, S. K., Ochi, T., and Morita, I., "Two-Dimensional Water Jet Impinging for Cooling of High Temperature Plate," *Transactions of the Japan Society of Mechanical Engineers*, Ser. B, Vol. 46, No. 404, 1980, pp. 714–724.

[18]Liu, Z. H., and Wang, J., "Study on Film Boiling Heat Transfer for Water Jet Impinging on a High Temperature Flat Plate," *International Journal of Heat and Mass Transfer*, Vol. 44, No. 13, 2001, pp. 2475–2481.

[19]Spiegler, P., Hopenfeld, J., Silberberg, M., Bumpus, C. F., and Norman, A., "Onset of Stable Film Boiling and the Foam Limit," *International Journal of Heat and Mass Transfer*, Vol. 6, No. 5, 1963, pp. 987–994.

[20]Segev, A., and Bankoff, S. G., "The Role of Adsorption in Determining the Minimum Film Boiling Temperature," *International Journal of Heat and Mass Transfer*, Vol. 23, No. 4, 1980, pp. 637–642.

[21]Zuber, N., "Hydrodynamic Aspects of Boiling Heat Transfer," U.S. Atomic Energy Commission Rept. AECU-4439, Univ. of California, Los Angeles, CA, 1959.

[22]Berenson, P. J., "Film Boiling Heat Transfer Form a Horizontal Surface," *Journal of Heat Transfer*, Vol. 83, No. 2, 1961, pp. 351–362.

[23]Lienhard, J. H., and Wang, P. T. Y., "The Dominant Unstable Wavelength and Minimum Heat Flux During Film Boiling on a Horizontal Cylinder," *Journal of Heat Transfer*, Vol. 86, No. 2, 1964, pp. 220–226.

[24]Lienhard, J. H., and Dhir, V. K., "On the Predication of the Minimum Pool Boiling Heat Transfer," *Journal of Heat Transfer*, Vol. 102, No. 3, 1980, pp. 457–460.

[25]Bromley, L. A., Leroy, N. R., and Robbers, J. A., "Heat Transfer in Forced Convection Film Boiling," *International Engineering Chemistry*, Vol. 45, No. 1, pp. 2639–2646.

[26]Rohsenow, W. M., and Choi, H. Y., *Heat, Mass and Momentum Transfer*, 1st ed., Prentice–Hall, Englewood Cliffs, NJ, 1961, pp. 146–150.

[27]Nishio, S., "Prediction Technique for Minimum-Heat-Flux-Point Condition of Saturated Pool Boiling," *International Journal of Heat and Mass Transfer*, Vol. 30, No. 10, 1987, pp. 2045–2057.